


 Cite this: *Chem. Commun.*, 2021, 57, 11213

 Received 20th July 2021,
 Accepted 1st October 2021

DOI: 10.1039/d1cc03906g

rsc.li/chemcomm

Predicting the impact sensitivity of a polymorphic high explosive: the curious case of FOX-7†

 Adam A. L. Michalchuk,^a Svemir Rudić,^b Colin R. Pulham^c and Carole A. Morrison^{*c}

The impact sensitivity (IS) of FOX-7 polymorphs is predicted by phonon up-pumping to decrease as layers of FOX-7 molecules flatten. Experimental validation proved anomalous owing to a phase transition during testing, raising questions regarding impact sensitivity measurement and highlighting the need for models to predict IS of polymorphic energetic materials.

Understanding molecular mechano-chemical reactivity has been the focus of research into energetic materials (EMs) for over 75 years.¹ EMs are able to convert mechanical energy into a chemical response, thereby resulting in their widespread uses across military and civilian applications. From a technological perspective, the response of EMs to mechanical impact – impact sensitivity (IS) – is arguably the most critical parameter. EMs which initiate under mild impact (*i.e.* are sensitive) pose great risk to safety and are often not suitable for real-world applications. Determining the IS of new EMs is paramount to developing new materials with targeted applications.

Established IS testing protocols are based on the drop-hammer approach, but are known to produce widely varying results. These variations derive from numerous, often poorly controllable, experimental parameters, including particle size, defect concentration, and the presence of impurities. For example, the reported impact sensitivity of FOX-7 (1,1-diamino-2,2-dinitroethene, DADNE, Fig. 1) ranges from 11 J through to 30 J.² Understanding this variability is further complicated by literature reports quoting IS values in two different ways: (1) limiting impact energy, E_0 , below which no impacts lead to initiation, and (2) the energy at which 50% of impacts lead to initiation, E_{50} . Correspondingly, significant efforts have been devoted to establishing theoretical approaches to screen IS *in silico*.^{3–5}

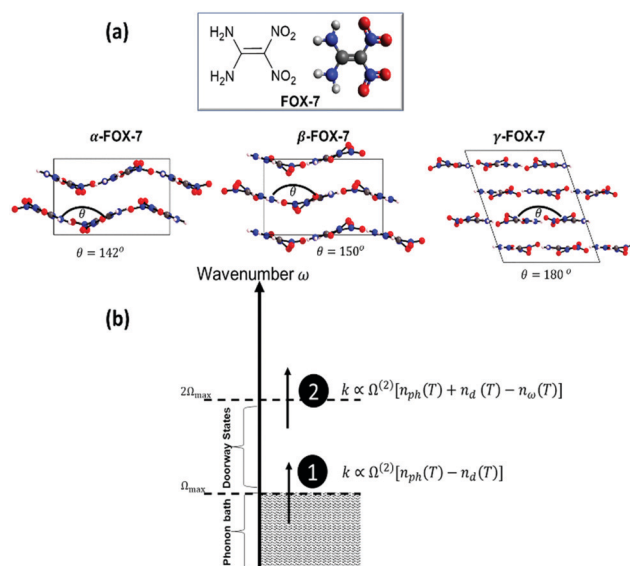


Fig. 1 Description of the model used in this work. (A) Chemical and crystallographic structures of FOX-7, including α -FOX-7 ($P2_1/n$); β -FOX-7 ($P2_12_12_1$) and γ -FOX-7 ($P2_1/n$). Atoms are coloured as (red) oxygen; (blue) nitrogen; (grey) carbon, and (white) hydrogen. (B) Mechanism of multi-phonon up-pumping. (1) Phonons scatter at a rate proportional to the two-phonon density of states $\Omega^{(2)}$ and the Planck–Einstein populations of the phonon (n_{ph}) and doorway modes (n_d). (2) Doorway states scatter upwards into molecular modes with populations n_ω . Further mathematical details are given in ESI,† S3 and ref. 17.

Theoretical screening methods have typically involved the study of isolated gas-phase molecules.⁶ Despite their predictive power, their simplicity renders gas-phase models unable to capture key experimental findings. Notably, EM mechano-chemical reactivity depends intimately on crystal packing,⁷ and varies across polymorphs⁸ and multi-component materials.⁹ Moreover, it is a well-known fact, albeit poorly understood, that EMs with layered crystal structures are generally less sensitive to mechano-chemical stimuli. This is exemplified by the prototypic insensitive layered EM, TATB (1,3,5-triamino-2,4,6-trinitro-benzene). It has been postulated that this decreased sensitivity stems from dissipation of

^a Federal Institute for Materials Research and Testing (BAM), Richard Wilstaetter Str 11, 12489, Berlin, Germany. E-mail: adam.michalchuk@bam.de

^b ISIS Neutron and Muon Source, STFC, Rutherford Appleton Laboratory, Chilton, Didcot, OX11 0QX, UK

^c EaStCHEM School of Chemistry and Centre for Science at Extreme Conditions, University of Edinburgh, EH9 3FJ, Edinburgh, UK.

E-mail: carole.morrison@ed.ac.uk

† Electronic supplementary information (ESI) available. See DOI: 10.1039/d1cc03906g



mechanochemical energy associated with slippage of the layers.^{10–12} However, as evidenced by the highly sensitive layered material, hexanitrobenzene, the extent of crystallographic layering and hence ease of slippage is not the complete story.¹³

Unfortunately, comparing the mechano-chemical reactivity of layered and non-layered EMs usually involves the study of two different energetic molecules. This makes it difficult to identify the origin of low sensitivity as being molecular or structural in nature. However, the thermally accessible polymorphs of FOX-7 offer an excellent route to bypass this problem, Fig. 1a. At ca. 115 °C the thermodynamically stable α -FOX-7 converts to β -FOX-7, and subsequently to γ -FOX-7 at ca. 173 °C.^{14,15} Importantly, the layers of FOX-7 molecules become increasingly flattened across these transitions. By combining advanced simulation and experiment we herein investigate how crystallographic packing in FOX-7 affects IS properties of the same energetic molecule. In doing so, we consider the reliability of standard testing protocol for measuring IS of polymorphic materials.

We have reported recently the development of a successful IS prediction model^{13,16,17} rooted in the fundamental concepts of vibrational energy transfer: phonon up-pumping.¹⁸ In this model, Fig. 1b and ESI,† S3, the mechanical impact superheats the crystal lattice vibrations *via* adiabatic compression. The equilibrated crystal temperature of an adiabatically compressed crystal long after impact, T_f , depends on the compression associated with the impact, V/V_0 , and the material Gruneissen parameter (γ),

$$\left(\frac{T_f}{T_0}\right) = \left(\frac{V_f}{V_0}\right)^{-\gamma} \quad (1)$$

The superheated phonon quasi-temperature (ϕ_p) that follows immediately after impact can be then obtained *via* both the bulk heat capacity (C) and the phonon heat capacity (C_{ph}),

$$C_{ph} [\phi_p - T_0] = \int_{T_0}^{T_f} dTC(T) \quad (2)$$

Phonon–phonon scattering facilitates the transfer of excess energy from the superheated phonon bath ($\omega < \Omega_{max}$) into localised molecular vibrations ($\omega > \Omega_{max}$). Assuming Einstein phonons, the rate of phonon up-pumping (τ) follows according to

$$\tau \propto V^{(3)} \delta(-\omega_1 - \omega_2 + \Omega) \quad (3)$$

where the Kronecker delta (δ) describes the two-phonon density of states ($\Omega^{(2)}$) in which the scattering of two phonons (ω_1 and ω_2) forms a third phonon of higher frequency (Ω). Following our previous model,¹⁷ ω_2 is restricted to values $< \Omega_{max}$ (*i.e.* at least one phonon must reside in the phonon bath). The strength of scattering is defined by the third order anharmonicity constant, $V^{(3)}$. Owing to the immense computational costs of calculating $V^{(3)}$ from first principles, our model adopts the average anharmonic approximation.¹⁹ This approximation posits that the magnitude of $V^{(3)}$ depends on the type of phonons involved, *i.e.* whether they are (q) external lattice modes, or (Q) internal molecular modes. For the scattering of any three phonons in eqn (3), the magnitude of $V^{(3)}$ follows as $qqq > qqQ > qQQ > QQQ$.¹⁸ Correspondingly, all states that are accessible by qqq interactions (*i.e.* all external mode

scattering) will equilibrate rapidly, establishing a ‘hot’ phonon bath. The excess energy in the phonon bath scatters upwards (qqQ processes) into the region $\Omega_{max} - 2\Omega_{max}$ (doorway states; Step 1 in Fig. 1b). To ensure momentum conservation, these qqQ processes are restricted to ‘overtone’-type scattering where $\omega_1 = \omega_2$. Finally, secondary scattering processes (qQQ) pump energy to $\omega > 2\Omega_{max}$ (Step 2 in Fig. 1b) by any available combination of ω_1 and ω_2 . The amount of energy which eventually occupies this region is then available to induce chemistry *via* heightened vibrational excitation. This is the onset of EM initiation.

To explore an up-pumping based model of IS for the FOX-7 polymorphs using our recent developments,¹⁷ we computed the zone-centre (Γ -point) phonon spectra, Fig. 2a, for each of the polymorphic forms at the PBE-D2 level of Density Functional Theory (see full computational details in ESI,† S1). Additionally, we successfully prepared a sample of γ -FOX-7 according to the procedures reported by Crawford *et al.*¹⁴ It was therefore possible to measure inelastic neutron scattering (INS) spectra for each of α - and γ -FOX-7 against which to validate our DFT models. Unfortunately, attempts to prepare stable samples of β -FOX-7 were not successful, with the sample reverting to α -FOX-7 upon cooling. Our

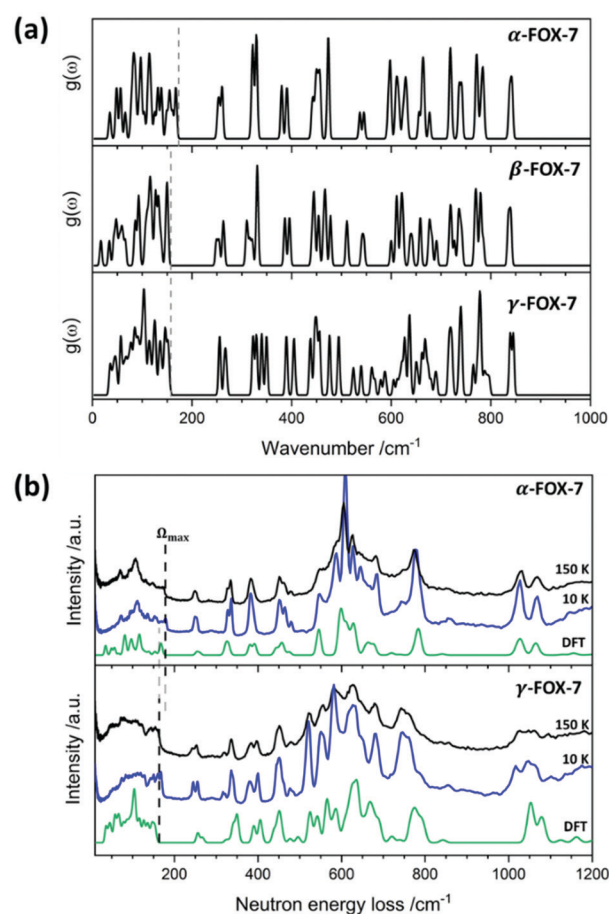


Fig. 2 Vibrational structure of FOX-7 polymorphs. (A) Calculated Γ -point phonon spectra (Gaussian smearing 5 cm^{-1}) for the three polymorphic forms. (B) Inelastic neutron scattering spectra for α - and γ -FOX-7. Experimental lines for (blue) 10 K and (black) 150 K are shown alongside (green) simulated spectra. Vertical dotted lines mark the top of the phonon bath.



Table 1 Key features in the vibrational structure of FOX-7 polymorphs. The top of the phonon bath (Ω_{\max}) and doorway density of phonon states (DOPS) are given

	Polymorphic form		
	α	β	γ
$\Omega_{\max}/\text{cm}^{-1}$	175	160	160
DOPS/ 10^{-2}	1.71	1.14	0.66
$C_{\text{ph}}/\text{J K}^{-1} \text{mol}^{-1}$	68.57	68.57	72.72
$C_{\text{tot}}/\text{J K}^{-1} \text{mol}^{-1}$	342.76	342.43	346.63
$C_{\text{ph}}/C_{\text{tot}}$	5.00	5.00	4.77
$T_{\text{shock}}/\text{K}$	3278.0	3278.0	3120.7

DFT models reproduced the INS spectra well, but appear to routinely slightly underestimate the value of Ω_{\max} for each polymorph as compared with the low temperature (10 K) INS spectra, Fig. 2b (α -FOX-7 exp (10 K) = 182 cm^{-1} , DFT-D = 175 cm^{-1} ; γ -FOX-7 exp (10 K) = 172 cm^{-1} , DFT-D = 160 cm^{-1}). Reassuringly, INS spectra collected at elevated temperatures (150 K) show a softening of Ω_{\max} with no change in vibrational bands at higher wavenumbers. Hence, we can conclude that our simulated spectra agree well with the vibrational spectra of FOX-7 polymorphs under realistic testing conditions, thereby validating the vibrational frequencies used for our up-pumping model.

The vibrational spectra are similar for all three polymorphs, but with one striking variation. As the layers of FOX-7 molecules flatten in the crystal structure, the frequency of the vibrational bands at the top of the phonon bath (Ω_{\max}) soften – see Table 1 and Fig. 2a. This reflects a decrease in the strength of the interlayer interactions. According to eqn (3), a decrease in Ω_{\max} has the effect of reducing the number of states accessible through qqQ coupling, thereby reducing the rate of up-pumping. For a unit cell comprising Z molecules, the relative rate of up-pumping is reflected in the density of phonon states ($\text{DOPS} \approx (Z\Omega_{\max})^{-1} \int_{\Omega_{\max}}^{2\Omega_{\max}} g(\omega) d\omega$) in the doorway region, which for the polymorphs of FOX-7 scale as α -FOX-7 > β -FOX-7 > γ -FOX-7, see Table 1 and ESI,† S4. This in turn suggests two potential structural features for tuning the sensitivities of EMs. While the decrease in DOPS from α to β -FOX-7 is a direct reflection of the softening of Ω_{\max} , the further decrease from β to γ FOX-7 likely corresponds to an increase in Z (*i.e.* the number of energy-absorbing molecules; see crystal structures in Fig. 1a). Similar correlations based on DOPS for molecular EMs have been previously suggested.^{13,20,21}

We explore further the prediction of IS for FOX-7 polymorphs using the complete vibrational up-pumping model. From our simulated vibrational frequencies, values for bulk C_{tot} and phonon bath C_{ph} were calculated, Table 1 and ESI,† S4, and the initial conditions for ϕ_{ph} were derived from their ratio, eqn (2). In the high temperature limit, each vibration contributes $k_{\text{B}}T$ to C_{tot} . Correspondingly, the theoretical heat capacity for each polymorph is expected to be equal. The small discrepancy observed in our case does not however affect the up-pumping simulations (see ESI,† S5). Our up-pumping calculations were performed using the two-step model outlined in Fig. 1b, at a bulk equilibrium temperature of 300 K. The resulting relative IS for the three FOX-7 polymorphs are shown in Fig. 3, alongside the corresponding values for a range of

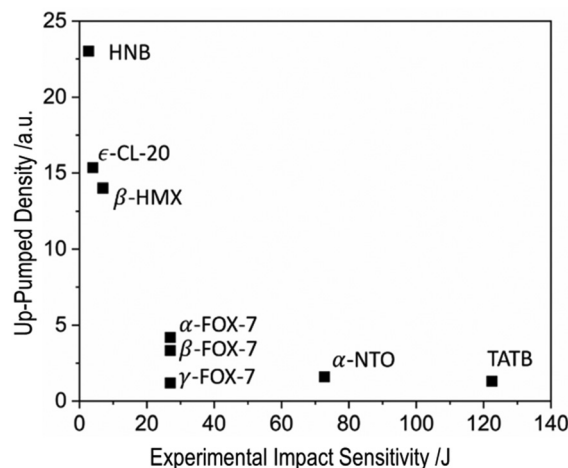


Fig. 3 Multi phonon up-pumped values for three FOX-7 polymorphs and a range of well-known EMs taken from ref. 17. A full description of the simulated FOX-7 values is given in ESI,† S5. In the absence of available data, the three polymorphs of FOX-7 have been plotted at the experimental sensitivity of α -FOX-7.

EMs that we have reported previously.¹⁷ Our predictions suggest that as layers of FOX-7 molecules become flattened, the sensitivity decreases. Moreover, the up-pumping prediction for γ -FOX-7 (which contains flat molecular layers) places it in line with the prototypical insensitive layered EM, TATB. From the success of our model, the reason for desensitisation of layered EMs becomes clear: given that our model only considers the up-pumping of energy through the vibrational DOS, it must be the changes in the vibrational DOS, induced by changes in the crystal packing, which alter the impact sensitivity metric.

To validate our up-pumping predicted IS, we attempted to measure the experimental values of IS for both the α - and γ -polymorphic forms. We note that the experimental IS of α -FOX-7 has been documented widely. Typical E_{50} values of 24–30 J are reported, although indications of IS as low as 10–11 J are also known.² To the best of our knowledge, drop hammer testing of γ -FOX-7 has not yet been reported. Here, samples of both α - and γ -FOX-7 were subjected to impact sensitivity testing using the BAM fall-hammer limiting impact ‘go/no-go’ criteria. Hence, our values are indicative of E_0 .

The sample of α -FOX-7 tested in this way (see ESI,† S6) suggested $E_0 \approx 8$ J. The significantly smaller initiation energy of E_0 versus E_{50} is expected. Contrary to up-pumping predictions, and to the widely held view that layered material are insensitive to impact, BAM fall hammer testing of γ -FOX-7 did not indicate reduced sensitivity as compared with the α -form. Instead, the same value of E_0 was obtained as for α -FOX-7, to within the experimental error of the measurement (see ESI,† S6).

To explore this paradox in further detail, samples of γ -FOX-7 which did not initiate upon impact were analysed by powder X-ray diffraction, and compared to simulated patterns of pure α - and γ -FOX-7, Fig. 4. Remarkably, all samples of γ -FOX-7 which were exposed to mechanical impact had converted back to the α -phase. In contrast, samples of γ -FOX-7 that were not exposed to testing did not convert, even after 72 hour storage under ambient conditions. Hence, the observed polymorphic



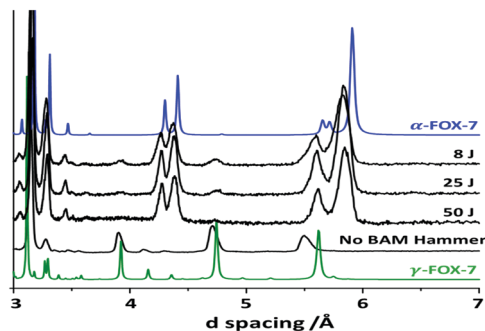


Fig. 4 PXRD profiles for FOX-7 before and after BAM hammer treatment (see ESI,† S6), with that for a sample stored at room conditions for three days without BAM Hammer testing. Simulated patterns for α -FOX-7 (blue) and γ -FOX-7 (green) are shown for comparison. Note a small offset in the position of the experimental peak of γ -FOX-7 at $d \approx 5.5$ Å, which corresponds to the crystallographic (0 0 2) plane. This offset is due to a minor misalignment of the diffractometer and sample geometry.

transformation did not result from handling or storage of γ -FOX-7. While we cannot discount entirely the role of defects or particle structure in dictating the observed sensitivity, we suggest that the seemingly identical IS values of the herringbone (α) and layered (γ) phases of FOX-7 were likely to be the result of an impact-induced phase transition. This transition may be the observed $\gamma \rightarrow \alpha$ phase transition or could include an intermediate layering of the α -phase upon impact; the latter is plausible given that the layering of FOX-7 is known to increase with pressure.²² Moreover, it remains unclear whether the impact, local heating, or interparticle friction is responsible for the transformation. Further shock compression studies are required to better understand this fascinating phenomenon. It is, however, clear that the results of current BAM fall hammer testing protocol should be interpreted with caution, particularly when dealing with polymorphic EMs. To the best of our knowledge this represents the first example of BAM hammer induced-polymorphism during IS testing. Given the wide-spread presence of polymorphism in EMs we do not expect this to be an isolated phenomenon.

In summary, we have explored the variation in impact sensitivity across three polymorphic forms of the high explosive FOX-7: α , β , and γ . Using a theoretical model based on vibrational up-pumping, we predict that the increased layering of the polymorphs reduces the impact sensitivity. This is consistent with trends in EM research which suggest that layered materials exhibit reduced sensitivity. Experimental validation of the up-pumping model was sought using BAM fall hammer testing. For the first time, the impact sensitivity of a sample of γ -FOX-7 was measured. However, in stark contrast to prevailing thought, and the up-pumping predictions reported herein, the layered γ -form exhibited an identical impact sensitivity as the herringbone α -form. *Ex situ* powder X-ray diffraction showed that γ -FOX-7 converts to the α -form under BAM fall hammer impact. We suggest this transition to be responsible for the seemingly paradoxical impact sensitivity results. Although this is the first reported case of a fall hammer-induced polymorphic transition, it is surely not an isolated case: the academic literature cites many examples of pressure-induced polymorphism in EMs.²³ Thus this work further highlights the need for robust theoretical platforms on which to

screen and explore mechano-chemical responses of EMs, in order that structure–property relationships are properly understood.

INS measurements were performed on the TOSCA^{24–26} instrument at ISIS Neutron and Muon Facility (RB1710382). The authors thank BAM IT for access to computational resources and to Dr D. Williamson (University of Cambridge) for access to the BAM Fall Hammer. We are also grateful for computational support from the United Kingdom Materials and Molecular Modelling Hub, which is partially funded by EPSRC (EP/P020194 and EP/T022213), for which access was obtained *via* the UKCP consortium and funded by EPSRC grant ref EP/P022561/1.

Conflicts of interest

There are no conflicts to declare.

References

- 1 R. B. Parlin, G. Duffy, R. E. Powell and H. Eyring, *The Theory of Explosion Initiation*, National Defense Research Committee of the Office of Scientific Research and Development, 1943.
- 2 W. Trzcinski and A. Belaada, *Cent. Eur. J. Energ. Mater.*, 2016, **13**, 527–544.
- 3 R. Tsyshevsky, O. Sharia and M. Kuklja, *Molecules*, 2016, **21**, 236.
- 4 S. V. Bondarchuk, *New J. Chem.*, 2019, **43**, 1459–1468.
- 5 D. Mathieu, *Ind. Eng. Chem. Res.*, 2017, **56**, 8191–8201.
- 6 B. M. Rice and J. J. Hare, *J. Phys. Chem. A*, 2002, **106**, 1770–1783.
- 7 Y. Ma, A. Zhang, X. Xue, D. Jiang, Y. Zhu and C. Zhang, *Cryst. Growth Des.*, 2014, **14**, 6101–6114.
- 8 B. Asay, B. Henson, L. Smilowitz and P. M. Dickson, *J. Energ. Mater.*, 2003, **21**, 223–235.
- 9 S. R. Kennedy and C. R. Pulham, in *Monographs in Supramolecular Chemistry*, ed. C. B. Aakeröy and A. S. Sinha, Royal Society of Chemistry, Cambridge, 2018, pp. 231–266.
- 10 Y. Ma, A. Zhang, C. Zhang, D. Jiang, Y. Zhu and C. Zhang, *Cryst. Growth Des.*, 2014, **14**, 4703–4713.
- 11 J. Zhang, L. A. Mitchell, D. A. Parrish and J. M. Shreeve, *J. Am. Chem. Soc.*, 2015, **137**, 10532–10535.
- 12 R. Bu, W. Xie and C. Zhang, *J. Phys. Chem. C*, 2019, **123**, 16014–16022.
- 13 A. A. L. Michalchuk, M. Trestman, S. Rudić, P. Portius, P. T. Fincham, C. R. Pulham and C. A. Morrison, *J. Mater. Chem. A*, 2019, **7**, 19539–19553.
- 14 M.-J. Crawford, J. Evers, M. Göbel, T. M. Klapötke, P. Mayer, G. Oehlinger and J. M. Welch, *Propellants, Explos., Pyrotech.*, 2007, **32**, 478–495.
- 15 J. Evers, T. M. Klapötke, P. Mayer, G. Oehlinger and J. Welch, *Inorg. Chem.*, 2006, **45**, 4996–5007.
- 16 A. A. L. Michalchuk, P. T. Fincham, P. Portius, C. R. Pulham and C. A. Morrison, *J. Phys. Chem. C*, 2018, **122**, 19395–19408.
- 17 A. A. L. Michalchuk, J. Hemingway and C. A. Morrison, *J. Chem. Phys.*, 2021, **154**, 064105.
- 18 D. D. Dlott and M. D. Fayer, *J. Chem. Phys.*, 1990, **92**, 3798–3812.
- 19 S. Califano, V. Schettino and N. Neto, *Lattice Dynamics of Molecular Crystals*, Springer-Verlag, Berlin, Heidelberg, 1981.
- 20 J. Bernstein, *J. Chem. Phys.*, 2018, **148**, 084502.
- 21 S. Ye, K. Tonokura and M. Koshi, *Combust. Flame*, 2003, **132**, 240–246.
- 22 S. Hunter, P. L. Coster, A. J. Davidson, D. I. A. Millar, S. F. Parker, W. G. Marshall, R. I. Smith, C. A. Morrison and C. R. Pulham, *J. Phys. Chem. C*, 2015, **119**, 2322–2334.
- 23 F. P. A. Fabbiani and C. R. Pulham, *Chem. Soc. Rev.*, 2006, **35**, 932.
- 24 D. Colognesi, M. Celli, F. Cilloco, R. J. Newport, S. F. Parker, V. Rossi-Albertini, F. Sacchetti, J. Tomkinson and M. Zoppi, *Appl. Phys. A: Mater. Sci. Process.*, 2002, **74**, s64–s66.
- 25 S. F. Parker, F. Fernandez-Alonso, A. J. Ramirez-Cuesta, J. Tomkinson, S. Rudic, R. S. Pinna, G. Gorini and J. Fernández Castañón, *J. Phys.: Conf. Ser.*, 2014, **554**, 012003.
- 26 R. S. Pinna, S. Rudic, S. F. Parker, M. Zanetti, G. Škoro, S. P. Waller, C. A. Smith, M. J. Capstick, D. J. McPhail, D. E. Pooley, G. D. Howells, G. Gorini and F. Fernandez-Alonso, *Nucl. Instrum. Methods Phys. Res., Sect. A*, 2018, **896**, 68–74.

